PAPER

Check for updates

Electrolyte and pH-sensitive amphiphilic alginate: synthesis, self-assembly and controlled release of acetamiprid†

Yiyuan Tang, [ID] Kai Chen, Jiacheng Li, [ID]* Yuhong Feng,* Gaobo Yu, Longzheng Wang, Xinyu Zhao, Yang Peng and Quan Zhang

In this study, a pH-responsive amphiphilic alginate (Ugi-Alg) was synthesized *via* Ugi reaction without using a catalyst. The structure of Ugi-Alg was confirmed by FT-IR and ^{1}H NMR spectroscopy. Amphiphilic alginate can form micelles in an aqueous medium due to it's amphiphilic nature.. The impacts of Na^+ concentration and pH on the micelle size were characterized by dynamic light scattering (DLS) and transmission electron microscopy (TEM). The dynamic light scattering observations showed that micelle size increases with the decrease in Na^+ concentration in aqueous solution. However, the micelle size decreases first and then increases as the pH value decreases from 5.3 to 2.0. Transmission electron microscopy confirmed that the mean size of micelles is 30–200 nm. In addition, a model hydrophobic pesticide (acetamiprid) was loaded in the micelles. The encapsulation efficiency and release behavior of micelles were studied, which could be controlled by Na^+ concentration and pH. The results indicated that encapsulation efficiency of acetamiprid increases from 55% to 96% due to the increase in Na^+ concentration from 0.01 M to 0.3 M. Moreover, with the decrease in pH from 5.3 to 2.0, encapsulation efficiency increases from 55% to 80%. Furthermore, the data of acetamiprid release kinetics could be well-fitted by the Weibull model.

1. Introduction

Pesticide use accounted for about 32 billion US$ by 2007,[1] and is expected to increase 2.7 times by 2050.[2] However, more than 90% of the applied conventional pesticides are either lost in the environment or never reach the target area required for pest control at the exact time and in precise quantities due to the nonspecific and periodic application of active agents.[3] The sprayed pesticide flows away from the plants to nearby land or rivers with storm water. Therefore, higher concentrations of pesticides have been used to achieve the desire effect of pest control, which consequently led to severe environmental damage. Misuse of pesticides will not only increase the costs, but also cause environmental pollution, enhancement of pest resistance and biodiversity reduction.[4] To overcome these drawbacks, increasing attention is being paid to the application of responsive polymer micelles in agriculture to reduce the usage of pesticides. Responsive polymer micelles have significant potential in improving the performance of pesticides by increasing their efficiency and safety and making them environmentally less harmful.[5,6]

In recent years, site-specific delivery has been extensively studied in the realm of medicine, but less attention has been given to the application of these adaptive materials in agriculture.[7] Phloem is the vascular tissue of plants, and plays the critical role of carrying nutrients and photosynthates. However, many plant pathogens can reside within the phloem (*i.e.*, phloem-limited pathogens), which are parasitic and introduce deadly crop diseases (*i.e.*, citrus Huanglong disease).[8] Moreover, while most plant tissues exist in a slightly acidic environment, phloem maintains higher, slightly alkaline pH.[9] Therefore, we can design polymeric micelles to meet the specific delivery needs of the phloem. These micelles must be (i) responsive to basic pH found in the phloem, (ii) small enough to enter the plant cell through cell wall junctions, and (iii) biodegradable to reduce the extent of accumulation over time. Additionally, these micelles would ideally be capable of encapsulating guest compounds, including hydrophobic and hydrophilic small molecules or drugs.[10]

Alginate as a polymer material can be extracted from brown algae and features biodegradability, biocompatibility, hydrophilicity, and non-immunogenicity. Therefore, alginate had been extensively investigated in the food industry, environmental engineering, drug delivery, and tissue engineering.[11–14] However, the application of sodium alginate in hydrophobic

Key Laboratory of Advanced Materials of Tropical Island Resources, Ministry of Education, College of Materials and Chemical Engineering, Hainan University, 58 Renmin Road, Haikou 570228, Hainan Province, China. E-mail: hn136.631@163.com; lijiacheng@hainu.edu.cn; ljcfyh@263.net; Tel: +86-13976105128

† Electronic supplementary information (ESI) available. See DOI: 10.1039/c8ra05503c

drugs has been restricted, mainly due to its strong hydrophilicity. For example, as control release material, the capacity of sodium alginate is deficient, which easily leads to burst release of the encapsulated drug.[15] Moreover, as a mucosal adhesion agent the adhesion force sodium alginate due to non-hydrophobic interactions is small.[16] Alginate can be modified by hydrophobic groups *via* Ugi reactions to improve its performance.[17] The modified alginate containing hydrophilic and hydrophobic blocks demonstrated self-assembly in aqueous solution to form micelles with a hydrophilic shell and a hydrophobic core.[18] When the amphiphilic polymer is exposed to hydrophobic solvents, it can form the opposite orientation, with the hydrophobic parts on the outside and hydrophilic parts on the inside.[19] Many external stimuli can change the disassembly or morphology of micellar aggregates.[20] Amphiphilicity combined with pH-response of modified alginate makes it a more promising micellar carrier.

Herein, we synthesized amphiphilic alginate with reference to a previous study.[21] The amphiphilic nature of alginate allows it to self-assemble into micelles, and was used to develop pH-responsive micelles for pesticide delivery.[22] Acetamiprid, a model hydrophobic drug, was encapsulated in the micelles. The encapsulation stability and pH-triggered release behavior were evaluated. We aimed to develop a novel pH-responsive delivery system to meet the specific delivery needs of the phloem.

2. Materials and methods

2.1 Materials

Sodium alginate (NaAlg), formaldehyde, octylamine, hydrochloric acid, sodium hydroxide, ethanol, NaCl, and pyrene (analytical grade) were all purchased from Aladdin Chemical Reagent Co., Ltd. (Shanghai, China). Cyclohexyl isocyanide (analytical grade) was purchased from J & K Technology Co. Ltd (Beijing, China). In addition, molecular masses of NaAlg ($M_w = 613\,308$ and $M_n = 394\,342$) were assessed by gel permeation chromatography.

2.2 Synthesis and characterization of Ugi-Alg

The synthesis of Ugi-Alg was performed based on a previous study,[21] as shown in Scheme 1. In this reaction, formaldehyde and octylamine are dehydrated to form an imine. Then, the imine and cyclohexyl isocyanide reacts to form a nitrile sulfonium ion, and the carboxylic acid ion of the alginate acid attacks the carbon atom of the isonitrile to generate the intermediate. Finally, a Mumm rearrangement occurs with an acyl transferring into the bis-amide.[23] The detailed processes are as follows. First, an unmodified alginate (2 g, 9.25 mmol) was dissolved in 80 mL of water at 35 °C. The solution was then gently stirred overnight to achieve homogeneity. Second, the pH of the solution was adjusted to 3.6 with the addition of 0.5 M HCl. Third, formaldehyde (0.05 g, 1.67 mmol), octylamine (0.17 g, 1.32 mmol), and cyclohexyl isocyanide (0.2 g, 1.83 mmol) were successively added to the solution. The solution was then stirred at 35 °C for 24 h. Finally, the reaction mixture

was diluted to 0.7 wt%, purified by dialyzing it against distilled water for 3 days, and subsequently freeze-dried. The chemical structure of Ugi-Alg was confirmed by ^{1}H NMR (D$_2$O, 25 °C) using a 400 MHz Bruker nuclear magnetic resonance spectrometer. The FTIR spectra of the sample were recorded on a Tensor27 Fourier transform infrared spectrometer. The FTIR spectra and ^{1}H NMR spectra are shown in Fig. 1. The thermogravimetric analysis (TGA) results of Ugi-Alg are shown in Fig. S1.†

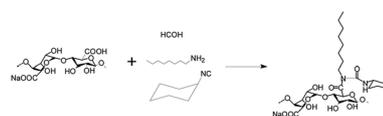### 2.3 Preparation of micelles

Ugi-Alg solutions were prepared by dissolving 5 mg of Ugi-Alg in 10 mL deionized water. They were stirred by a magnetic stirrer for 24 h. Then, the pH (2–5.3) and NaCl concentrations (0.01–0.3 M) of the solutions were changed. Consequently, the micelle solutions were obtained.

2.4 Characterization of Ugi-Alg micelles

The critical micelle concentration (CMC) of Ugi-Alg in aqueous media was determined using a fluorescence spectrophotometer. Fluorescence spectrophotometry was performed on a Hitachi F7000 fluorescence spectrophotometer using pyrene as the fluorescence probe. The excitation wavelength was set to 335 nm and the slit width was 2.5 nm. The fluorescence emission spectra were recorded in the range of 335 nm to 600 nm. All tests were performed at 25 °C. A 10 μL aliquot of 1.0×10^{-3} M pyrene was prepared in ethanol solvent and then added into a test tube. Then, ethanol was removed with the aid of nitrogen blowing. Subsequently, 5 g L^{-1} Ugi-Alg was added into the test tube with solutions of varying Ugi-Alg concentrations (0.001 g L^{-1} to 3.0 g L^{-1}). All sample solutions were shaken in a water bath overnight at room temperature to ensure that pyrene was completely entrapped in the hydrophobic micro-domains.

The zeta potential and z-average diameters of the Ugi-Alg micelles were measured by DLS with a Zetasizer Nano ZS90 (Malvern, UK). Ugi-Alg (1.0 g L^{-1}) was added into the test tube, and solutions of varying pH (2–5.3) and NaCl concentrations (0.01–0.3 M) were prepared. All sample solutions were shaken in a water bath overnight at room temperature. The analyzer adopts a He–Ne light source with 10 mW power, wavelength of 633 nm, scattering intensity measuring angle of 90°, and measuring temperature of 25 °C with an accuracy of ±0.1 °C.

The morphology of the Ugi-Alg micelles were observed using TEM (JEOL JEM-2010, Japan) at an acceleration voltage of 200 kV. A few drops of micelle solution were added on a carbon-coated copper grid. Negative staining was then performed by exposing the grid to 2 wt% tungsten–phosphoric acid solution, which was dried at room temperature. The average size of the micelles was calculated by Nano Measurer 1.2.

Scheme 1 The synthesis route of Ugi-Alg.

2.5 Preparation of acetamiprid-drug micelles

The preparation of acetamiprid/Ugi-Alg micelles is briefly described as follows. First, 5.0 g L^{-1} Ugi-Alg solutions was added to 1 mg mL^{-1} acetamiprid solutions (9 : 1, v/v). Then, they were mixed by a magnetic stirrer for 24 h. Then, varying pH (2–5.3) and NaCl concentrations (0.01–0.3 M) of the solutions were prepared. Consequently, acetamiprid-drug micelles were obtained.

To determine the encapsulation efficiency (EE), 2 mL supernatant of the acetamiprid-loaded micelle solution was centrifuged at a high speed (10 000 rpm) for 20 min and washed three times with a small amount of deionized water to remove the free acetamiprid. The concentrations of acetamiprid in the decanted aqueous solution and three times-washed solutions were analyzed by Waters e2695 high performance liquid chromatography (HPLC). The chromatographic conditions were as follows: FID detector, HP Hypsil C18 column (250 mm × 4.6 mm × 0.005 mm), mobile phase: methanol/water/acetonitrile (15 : 70 : 15, v/v/v), flow rate: 1 mL min^{-1}, column temperature: 40 °C. EE was calculated based on the following formula:

$$EE(wt\%) = \frac{A - B}{A} \qquad (1)$$

where A is the total amount of the acetamiprid, and B is the amount of acetamiprid remaining in the supernatant.

2.6 Controlled-release of the acetamiprid-loaded micelles

For the release experiment of acetamiprid from the micelles, 8 mL of the above micelles was put into a dialysis bag (cutoff molecular weight: 1000); then, the dialysis bag was introduced into a beaker containing 400 mL of distilled water. At predetermined time intervals (such as 10 min, 20 min, 30 min or 1 h, and 3 h), water was collected from the beaker and then, the dialysis bag was put into fresh 400 mL of distilled water. The acetamiprid concentration was determined by the abovementioned method. All studies were repeated two times and mean values were obtained.

3. Results and discussion

3.1 Synthesis of Ugi-Alg micelles

Sodium alginate was hydrophobically modified *via* the Ugi reaction. The FT-IR spectra of Alg and Ugi-Alg are presented in Fig. 1(a). From the FT-IR spectrum of Alg (Fig. 1(a)), the broad and strong peak at 3429.15 cm^{-1} is assigned to O–H stretching vibrations. It can be observed that a small peak appearing at 2926.48 cm^{-1} is attributed to C–H stretching vibrations of the saccharide structure. The characteristic peaks at 1620 and 1417 cm^{-1} are assigned to asymmetric and symmetric stretching vibrations of carboxylic acid (COO$^-$), respectively. After modification, the additional weak peaks observed at 2854 and 1385.14 cm^{-1} correspond to –CH$_2$– and –CH$_3$– bending vibrations of octyl and cyclohexyl, indicating the successful modification of NaAlg.[21,23] The weak peak at 1714 cm^{-1} may correspond to the C=O stretching vibrations of *N*-acylurea.

The ^{1}H NMR spectra of NaAlg and Ugi-Alg are presented in Fig. 1(b). The proton peaks ranging from 5.0 to 3.5 ppm are ascribed to the H of native alginate chains, including δ (ppm) = 5.08 (C1H, G unit) and 4.68 (C1H, M unit). Comparing the ^{1}H NMR spectrum of Alg with that of Ugi-Alg, some new proton peaks appear in the δ range from 2.0 to 0.5 ppm because of the presence of new functional groups linked to alginate. The proton assignments of the new functional groups are listed as follows: δ (ppm): 1.8–1.5 (t, 11H, C$_6$H$_{11}$ of cyclohexyl), 1.2 (s, 12H, (CH$_2$)$_6$ of octyl), 0.8 (s, 3H, CH$_3$ of octyl). According to these results, the conclusion can be drawn that Ugi-Alg was successfully synthesized.[21,24]

3.2 Assessment of Ugi-Alg micelles

3.2.1 Critical micelle concentration of Ugi-Alg. Polycyclic aromatic pyrene can be used as a fluorescent probe to explore the micro-environmental polarity of a micellar system. The
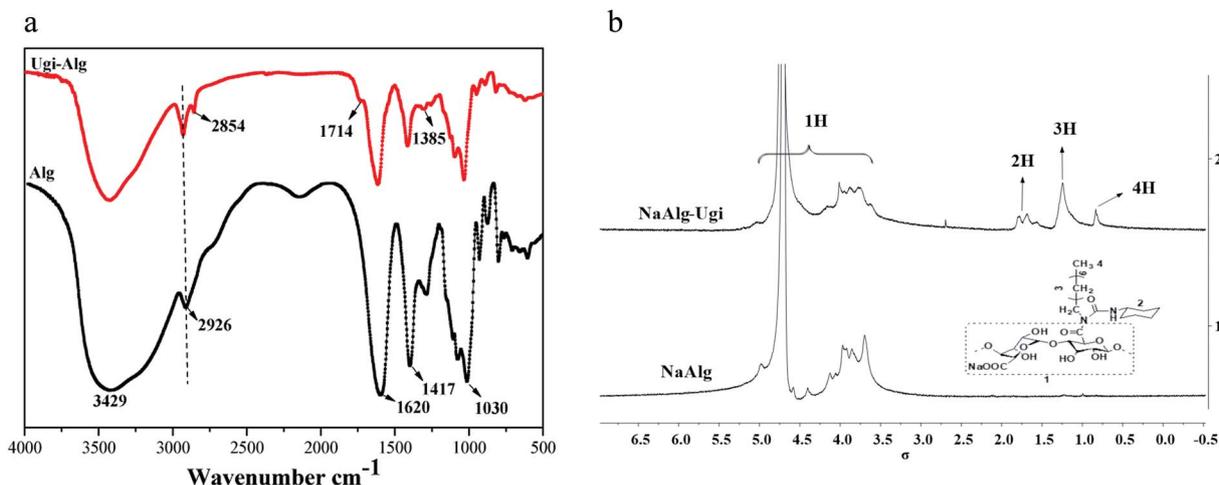

Fig. 1 (a) FT-IR spectrum (b) ^{1}H NMR spectrum of NaAlg and Ugi-Alg.
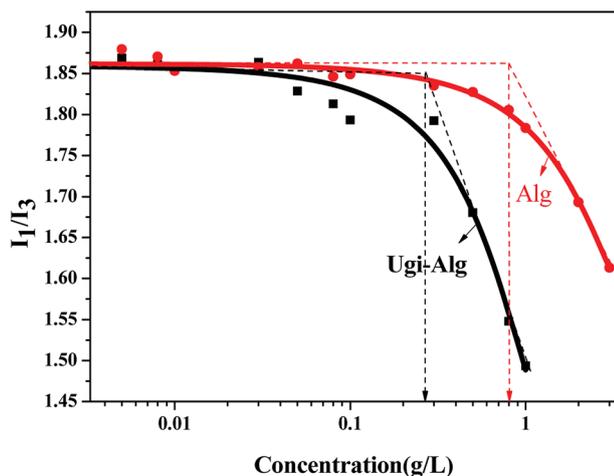
Fig. 2 Fluorescence spectra of NaAlg and Ugi-Alg.

fluorescence probe technique is efficient in examining the polyelectrolyte–surfactant interaction and degree of aggregation.[25] Hydrophobicity of hydrophobic alginates is described through critical aggregation concentration (CAC), which is detected by fluorescence measurements. According to the fluorescence analysis results (Fig. 2), the CMC of Ugi-Alg was 0.27 g L^{-1} in 0.01 M NaCl solution at pH = 5.3, while the CMC value of NaAlg was about 1 g L^{-1} under the same conditions. Ugi-Alg has stronger hydrophobicity than NaAlg, which makes it easier to form micelles at a lower concentration.

3.2.2 Effect of Na$^+$ concentration and pH on micelles structure. There are two main methods to form micelles of amphiphilic polymers, which include a direct dissolution method and a membrane-dialysis method. We executed the direct dissolution method to prepare the micelles. The zeta potential and z-average size of the Ugi-Alg micelles are shown in Fig. 3. Fig. 3(a) shows that as the Na$^+$ concentration decreased from 0.3 M to 0.01 M, the z-average size of micelles increased from 471.7 ± 18 nm to 967.3 ± 100 nm. A possible reason for this phenomenon is that with the increase in Na$^+$, an increasing number of ionic groups (COO$^-$) of polymer chains are shielded, so that the internal electrostatic repulsion

within the micelles is decreased. When the attractive forces due to hydrogen bonding or hydrophobic interactions overcomes the repulsion, the micelles are curled.[26–29] The zeta potential shown in Fig. 3(a) illustrates that the negative charge of the micelles surface decreased as Na$^+$ concentration increased.

Fig. 3(b) shows the effect of solution pH on zeta potential and z-average diameters of the Ugi-Alg micelles. With the decrease in pH value from 5.3 to 2.5, the micelles size decreased from 950 ± 45 nm to 218 ± 33 nm. Ngai et al.[30] reported that with the decrease in pH, an increasing number of anionic –COO$^-$ within the micelles were protonated to carboxylic groups (–COOH), resulting in a decrease in the internal electrostatic repulsion within the micelles. When the attractive forces due to hydrogen bonding or hydrophobic interactions overcomes the repulsion, the Ugi-Alg chains are curled, resulting in decreased micelles size. However, when the pH value decreased to 2.0, the micelles size increased, which may be because H$^+$ shielded the charge on the micelles' surface. As a result, the attractive forces resulting from hydrogen bonding or hydrophobic interactions overcome the inter-micelle repulsion, resulting in aggregation between micelles. An illustration of the Ugi-Alg aggregation in aqueous solution of different NaCl concentrations and pH values is exhibited in Scheme 2. The phenomenon was illustrated for the zeta potential of micelles (Fig. 3(b)).

3.2.3 Morphology of micelles. The submicroscopic structure with diameters less than 200 nanometers could be observed by transmission electron microscopy. The morphology of the micelles is shown in Fig. 4. To further support the abovementioned conclusions, amphiphilic alginate has been reported to form self-assembled micelles in the aqueous media.[31] Moreover, the size of the micelles decreased from 200 ± 6.3 nm to 50 ± 5.5 nm as the Na$^+$ concentration increased from 0.05 M to 0.3 M. With the increase in pH value from 5.3 to 2.0, the size of the micelles decreased from 150 ± 5.13 nm to 30 ± 3.5 nm, and then increased to 60 ± 4.3 nm. Interestingly, compared with the DLS data, the micelles diameter is much smaller. The reason may be that micelles are easy to swell in aqueous solution. The swelling ratio was calculated by using the following equation:
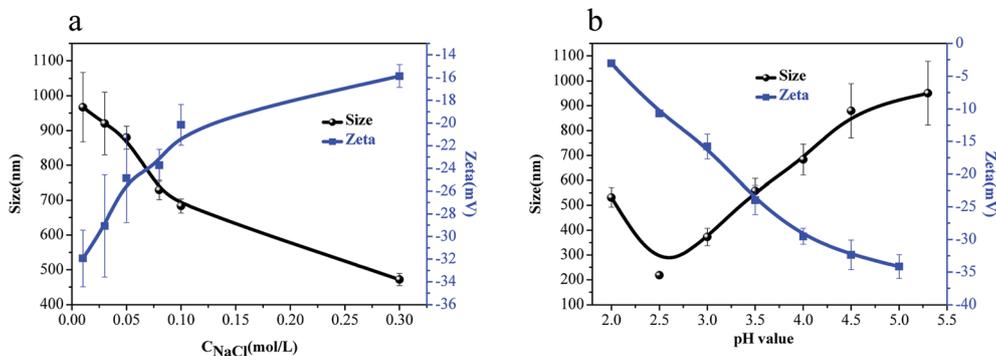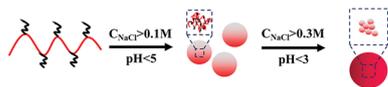

Fig. 3 (a) Effect of Na$^+$ concentration on the z-average diameters and zeta potentials of 1.0 g L^{-1} Ugi-Alg solution at pH = 5.3. (b) Effect of pH on the z-average diameters and zeta potentials of 1.0 g L^{-1} Ugi-Alg in 0.01 M aqueous NaCl solution.

Scheme 2 Schematic of Ugi-Alg aggregation in aqueous solution of different NaCl concentrations and pH values.

$$\text{Swelling ratio} = \frac{d_i - d_s}{d_s} \qquad (2)$$

where d_s is the diameter of dried micelles and d_i is the diameter of micelles in the solution.

As shown in Fig. 5, with the increase in Na^+ concentration, the swelling ratio increased, indicating that more the Na^+ concentration, the stronger would be the hydrogen bonding and hydrophobic interactions which will overcome the repulsion and form smaller micelles. The swelling ratio with varying pH values had similar trends with varying Na^+ concentration.

3.3 Controlled drug release of micelles

Acetamiprid was introduced for agricultural control of sucking-type insects on leafy vegetables, fruits and tea trees in the early 90s. However, acetamiprid has demonstrated high toxicity, causing potential risk to humans who are exposed to the contaminated environment.[32] Therefore, in our study, for minimizing this risk, we encapsulated acetamiprid with the appropriate polymers. The benefits of micelles include improvement of long-time efficiency and a controlled release of acetamiprid in the phloem.

The effects of different pH and Na^+ concentrations in solution on the encapsulation efficiency of acetamiprid were evaluated, as shown in Table 1. For the 0.01 M NaCl solution, varying the pH value from 5.3 to 2.0 caused a significant

increase in encapsulation efficiency of acetamiprid from 55% to 80%. Under the same pH solution, increasing the Na^+ concentration from 0.01 M to 0.3 M resulted in the distinct increase in encapsulation efficiency of acetamiprid from 55% to 96%. The most likely reason for this is that with the decrease in pH or increase in Na^+ concentration, the attractive forces due to hydrogen bonding or hydrophobic interactions overcome the repulsion and create a microenvironment, resulting in the significantly enhanced encapsulation efficiency of acetamiprid.[33]

Release profiles of acetamiprid from micelles were studied, as shown in Fig. 6. In general, within the first 100 min, a rapid drug release process occurred; then, the release rate became slower and displayed prolonged behavior. Interestingly, cumulative release of acetamiprid reached 80% in pH = 5.3 solution at 100 min. The reason may be that non-encapsulated acetamiprid first releases quickly from the dialysis membrane. Then, the encapsulated acetamiprid releases slowly, due to which the release rate becomes slower and displays prolonged behavior. As shown in Fig. 6(a), with the increase in the pH from 2.0 to 5.3, the release rate also increased. However, the release rate decreased as the Na^+ concentration increased. This is explained on the basis of the fact that because of the decrease in pH or increase in Na^+ concentration, resulting in the increasing strength of hydrogen bonding and hydrophobic interaction, swelling rate of micelles decreases (Fig. 5), leading to slower release rate.

To investigate the effect of pH and Na^+ concentration on the mechanism of acetamiprid release from micelles, a classical model, known as the Weibull model[31] was used:

$$\ln(\ln(1/(1 - F))) = b \ln t + \ln a \qquad (3)$$

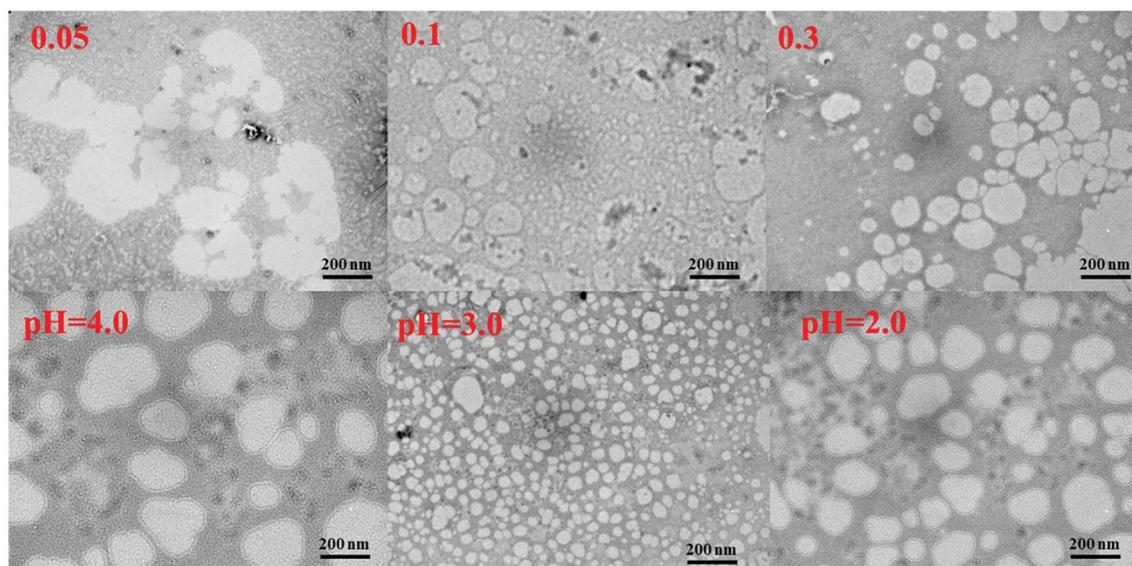where F and t are cumulative release and time, respectively, and a and b are constants.

Fig. 4 TEM images of 1.0 g L^{-1} Ugi-Alg micelles with pH = 5.3 at various NaCl concentrations: (a) 0.05 M, (b) 0.1 M and (c) 0.3 M. TEM images of 1.0 g L^{-1} Ugi-Alg micelles in 0.01 M NaCl solution with different pH values: (d) pH = 2.0, (e) pH = 3.0 and (f) pH = 4.0.
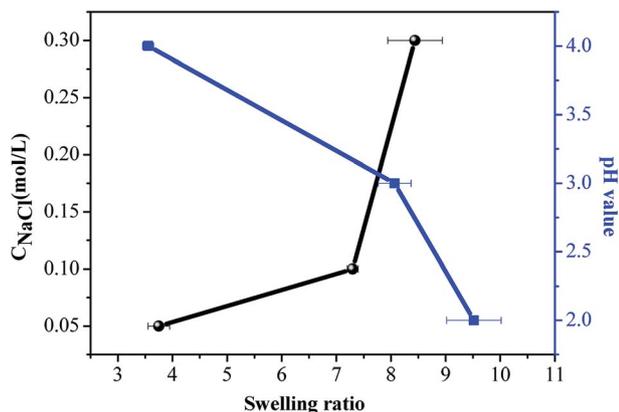
Fig. 5 The swelling ratio of micelles in the various pH value and Na$^+$ concentration solution.

Table 1 Effect of pH and Na$^+$ concentration solution on encapsulation efficiency of acetamiprid

pH value	NaCl concentration (M)	Encapsulation efficiency (%)
2.0	0.01	80%
3.0	0.01	70%
4.0	0.01	57%
5.3	0.01	55%
5.3	0.1	67%
5.3	0.3	96%

Papadopoulou et al.[34] reported that values of b lower than 0.75 denote that the release follows Fickian diffusion either in Euclidian ($0.69 < b < 0.75$) or in fractal space ($b < 0.69$). Moreover, for Fickian diffusion the increase in b reflects the decrease in the medium disorder. Values of b in the range of 0.75–1.0 indicate that the release is suitable for a combined mechanism (Fickian diffusion and Case II transport). The specific case when $b = 1$ is compatible with first-order release, where the concentration gradient in the dissolution medium drives the rate of release. Finally, when $b > 1$, a complex mechanism governs the release process. In fact, the release rate initially increases nonlinearly up to the inflection point and then decreases asymptotically.

By applying least-squares method to release data, the fitting curves were obtained (Fig. 6(b)), and the values of R2, b and the mechanism were estimated (Table 2). As can be seen from Table 2, R2 of all samples was about 0.97, indicating that the samples are suitable for the Weibull model. For 0.01 M Na$^+$ concentration, as the pH value is varied from 2.0 to 3.0 to 5.3, the value of b is 0.7615, 0.6554, and 0.7879, respectively, indicating that the mechanism of release changes from combined mechanism to Fickian and again to combined mechanism. When pH = 5.3, the values of b were found to vary from 0.2042 to 0.2088 when the Na$^+$ concentration varied from 0.1 M to 0.3 M, respectively. This indicates that under such circumstances, the release of acetamiprid followed the Fickian mechanism.
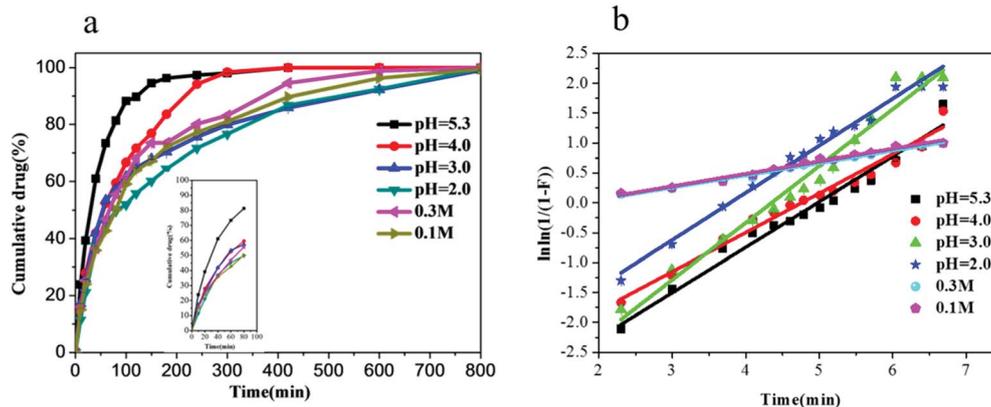

Fig. 6 (a) Release profiles of acetamiprid in various pH values and Na$^+$ solutions; (b) fitting curves of Weibull model in the various pH values and Na$^+$ concentration solutions.

Table 2 Comparison of the Weibull model data

pH value	NaCl concentration (M)	Weibull model		Mechanism
		R^2	B	
2.0	0.01	0.9723	0.7615 ± 0.1118	Combined mechanism (Fickian and case II transport)
3.0	0.01	0.9758	0.6554 ± 0.1087	Fickian diffusional mechanism
4.0	0.01	0.9640	0.9518 ± 0.0289	Combined mechanism (Fickian and case II transport)
5.3	0.01	0.9795	0.7879 ± 0.0838	Combined mechanism (Fickian and case II transport)
5.3	0.1	0.9894	0.2042 ± 0.0030	Fickian diffusional mechanism
5.3	0.3	0.9832	0.2088 ± 0.0030	Fickian diffusional mechanism

4. Conclusion

In this study, amphiphilic alginate (Ugi-Alg) was synthesized *via* the Ugi reaction without the aid of a catalyst and with inherent high atom economy and chemical yield. The structure of Ugi-Alg was confirmed by TGA, FT-IR and ^{1}H NMR spectrometry analyses. A series of experimental analyses (fluorescence spectroscopy, DLS and TEM) indicated that Ugi-Alg can self-assemble in water. Moreover, the size of micelles first decreased and then increased as the pH decreased from 5.3 to 2.0. With the increase in Na^+ concentration, the micelles size decreased. Interestingly, a high encapsulation efficiency of acetamiprid in the 0.3 M Na^+ concentration and pH = 5.3 solution was achieved, reaching up 96.4%. The release behavior of acetamiprid from the micelles could be controlled by changing the Na^+ concentration and pH solution. The mechanism of acetamiprid release was found to vary from combined to Fickian and again to combined mechanism when the pH varied from 2.0 to 5.3. When the Na^+ concentration was varied from 0.1 to 0.3 M, all systems exhibited Fickian mechanism. Consequently, this research implied that our strategy would potentially be an effective method to suit the specific delivery needs of the phloem.

Conflicts of interest

There are no conflicts to declare.

Acknowledgements

References

1 S. Sharma, S. Singh, A. K. Ganguli and V. Shanmugam, *Carbon*, 2017, **115**, 781–790.

2 D. Tilman, J. Fargione, B. Wolff, C. D'Antonio, A. Dobson, R. Howarth, D. Schindler, W. H. Schlesinger, D. Simberloff and D. Swackhamer, *Science*, 2001, **292**, 281–284.

3 L. D. Cao, H. R. Zhang, C. Cao, J. K. Zhang, F. M. Li and Q. L. Huang, *Nanomaterials*, 2016, **6**, 126.

4 D. Tilman, K. G. Cassman, P. A. Matson, R. Naylor and S. Polasky, *Nature*, 2002, **418**(6898), 671.

5 C. Sun, K. Shu, W. Wang, Z. Ye, T. Liu and Y. Gao, *Int. J. Pharm.*, 2014, **463**, 108–114.

6 R. Tasmin, Y. Shimasaki, M. Tsuyama, X. Qiu, F. Khalil and N. Okino, *Environ. Sci. Pollut. Res.*, 2014, **21**, 1064–1070.

7 S. J. Sonawane, R. S. Kalhapure and T. Govender, *Eur. J. Pharm. Sci.*, 2017, **99**, 45–65.

8 J. M. Bove and M. Garnier, *Plant Sci.*, 2002, **163**, 1083–1098.

9 J. W. Torpey, E. A. Komives, J. Kehr and J. I. Schroeder, *Plant J.*, 2008, **54**, 249–259.

10 M. R. Hill, E. J. MacKrell, C. P. Forsthoefel, S. P. Jensen, M. S. Chen, G. A. Moore, Z. L. He and B. S. Sumerlin, *Biomacromolecules*, 2015, **16**, 1276–1282.

11 G. Lawrie, I. Keen, B. Drew, A. Chandler-Temple, L. Rintoul and P. Fredericks, *Biomacromolecules*, 2007, **8**, 2533–2541.

12 Q. Li, C. G. Liu, Z. H. Huang and F. F. Xue, *J. Agric. Food Chem.*, 2010, **59**, 1962–1967.

13 P. Gurikov, S. Raman, D. Weinrich, M. Fricke and I. Smirnova, *RSC Adv.*, 2015, **11**, 7812–7818.

14 L. Yang, J. Guo, J. Wu and Y. Yang, *RSC Adv.*, 2017, **7**(80), 50626–50633.

15 B. L. Yao, Q. Li, X. Ma and C. H. Ni, *Chin. J. Spectrosc. Lab.*, 2009, **26**, 119–121.

16 L. F. Zhang, S. L. Song, H. Liang and A. G. Ji, *Chin. J. Biochem. Pharm.*, 2009, **30**, 281–284.

17 L. N. Hassani, F. Hendra and K. Bouchemal, Auto-associative amphiphilic polysaccharides as drug delivery systems, *Drug Discovery Today*, 2012, **17**(11–12), 608–614.

18 S. Menon, R. Thekkayil, S. Varghese and S. Das, *J. Polym. Sci., Part A: Polym. Chem.*, 2011, **49**(23), 5063–5073.

19 R. Trivedi and U. B. Kompella, *Nanomedicine*, 2010, **5**, 485–505.

20 J. Dong, Y. Wang, J. Zhang, H. Yang and G. Wang, *Soft Matter*, 2013, **9**, 370–373.

21 H. Q. Yan, X. Q. Chen, J. C. Li, Y. H. Feng, Z. F. Shi, X. H. Wang and Q. Lin, *Carbohydr. Polym.*, 2016, **136**, 757–763.

22 S. Chen, F. Jiang, Z. Cao and G. Wang, *Chem. Commun.*, 2015, **51**, 12633–12636.

23 M. S. Islam and M. R. Karim, *Colloids Surf., A*, 2010, **366**, 135–140.

24 K. Cho, X. Wang, Z. Chen and D. Shin, *Clin. Cancer Res.*, 2008, **14**, 1310–1316.

25 B. Y. Ren, Y. M. Gao, L. Lu, X. X. Liu and Z. Tong, *Carbohydr. Polym.*, 2006, **66**, 266–273.

26 W. L. Liu, W. Liu, A. Ye, S. F. Peng, F. Q. Wei, C. M. Liu and J. Z. Han, *Food Chem.*, 2016, **196**, 396–404.

27 H. V. Sæther, H. K. Holme, G. Maurstad, O. Smidsrød and B. T. Stokke, *Carbohydr. Polym.*, 2008, **74**, 813–821.

28 T. Schmelz, U. Lesmes, J. Weiss and D. J. McClements, *Food Hydrocolloids*, 2011, **25**, 1181–1189.

29 X. N. Shi, W. B. Wang and A. Q. Wang, *Carbohydr. Polym.*, 2013, **94**, 449–455.

30 H. A. Ngai and S. H. Behrens, *Macromolecules*, 2006, **39**, 8171–8177.

31 J. S. Yang, Q. Q. Zhou and W. He, *Carbohydr. Polym.*, 2013, **92**, 223–227.

32 R. Rapini, A. Cincinelli and G. Marrazza, *Talanta*, 2016, **161**, 15–21.

33 H. Wei, S. X. Cheng, X. Z. Zhang and R. X. Zhuo, *Prog. Polym. Sci.*, 2009, **34**, 893–910.

34 V. Papadopoulou, K. Kosmidis, M. Vlachou and P. Macheras, *Int. J. Pharm.*, 2006, **309**, 44–50.